Analysis of Microstrip-Like Transmission Lines by Nonuniform Discretization of Integral Equations

EIKICHI YAMASHITA, MEMBER, IEEE, AND KAZUHIKO ATSUKI

Abstract—**The nonuniform discretization of the integral equation on the tangential electromagnetic (EM) field on the boundary surface is proposed as a numerically efficient method to analyze the microstrip-like transmission lines. The calculated results of the propagation constant of the microstrip line based on this method are compared with other published analytical results. Various types of planar striplines are treated by the same formulas. The dominant and higher order modes of a shielded microstrip line are discussed and compared with the longitudinal-section electric (LSE) and linear synchronous motor (LSM) modes of a two-medium waveguide.**

I. Introduction

In the early stage of microstrip-line analyses, the TEM approximation was effectively employed to calculate the line capacitance as a basic parameter of the inhomogeneous transmission line [1]–[4]. Though this approximation was useful in a wide range of frequencies, more rigorous analytical methods have been explored to find its theoretical limitations [5]–[8]. The dispersion characteristics of the microstrip line at high frequencies, for example, have been reported by many papers. However, published numerical values even on the same problem are not necessarily in good agreement.

This paper describes a straightforward and numerically effective method to compute characteristic values of microstrip-like transmission lines. The main features of this method are the formulation of integral equations for general structures in a form of Zysman and Varon [7] and the derivation of the solution by the nonuniform discretization of the integrals. Numerical results based on this method are compared with other data [8]–[11] and empirical formulas [12]–[14]. The treatments of coplanar striplines [15], [16], shielded slot lines [17], and microstrip lines are shown. The dominant and higher order modes of microstrip lines are also discussed compared with the LSE and LSM modes of a two-medium waveguide.

II. Formulation of Integral Equations

Fig. 1 shows a microstrip-like transmission line which contains three dielectric layers, multistrip conductors, and a metallic shield enclosure. The strip conductors are assumed to be negligibly thin and the line lossless.

A hybrid-mode analysis is apparently necessary in this inhomogeneous structure. When the scalar potentials for TM waves and TE waves are defined by $\psi^{(e)}$ and $\psi^{(h)}$, respectively, the electromagnetic (EM) fields of hybrid modes [18] are given by

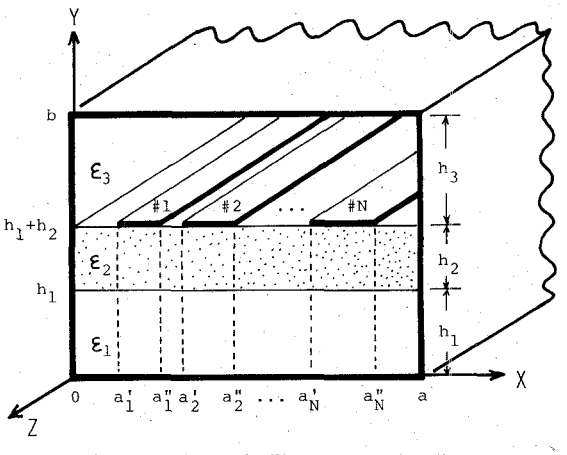

Fig. 1. Microstrip-like transmission line.

$$E_{zi} = j\frac{k_i^2 - \beta^2}{\beta}\psi_i^{(e)}(x,y)e^{-j\beta z} \tag{1a}$$

$$H_{zi} = j\frac{k_i^2 - \beta^2}{\beta}\psi_i^{(h)}(x,y)e^{-j\beta z} \tag{1b}$$

$$\boldsymbol{E}_{ti} = \nabla_t\psi_i^{(e)}(x,y)e^{-j\beta z} - \frac{\omega\mu_0}{\beta}\boldsymbol{a}_z \times \nabla_t\psi_i^{(h)}(x,y)e^{-j\beta z} \tag{1c}$$

$$\boldsymbol{H}_{ti} = \nabla_t\psi_i^{(h)}(x,y)e^{-j\beta z} + \frac{\omega\varepsilon_i}{\beta}\boldsymbol{a}_z \times \nabla_t\psi_i^{(e)}(x,y)e^{-j\beta z}, \quad i = 1,2,3 \tag{1d}$$

where ω is the angular frequency, μ_0 is the magnetic permeability of a vacuum, ε_i is the permittivity in the ith medium ($i = 1,2,3$), k_i is $\omega\sqrt{\varepsilon_i\mu_0}$, the subscript t denotes the transverse direction, $\boldsymbol{a}_z$ is the z-directed unit vector, and β is the unknown phase constant of the hybrid mode.

The general solution of the wave equation in each dielectric layer can be obtained by the method of the separation of variables. After applying the boundary conditions on the surface of the shielding conductor to the general solution, one obtains the following form:

$$\psi_1^{(e)} = \sum_{n=1}^{\infty} A_n^{(e)} \sinh(\alpha_n^{(1)}y)\sin(a_n x) \tag{2a}$$

$$\psi_2^{(e)} = \sum_{n=1}^{\infty} \{B_n^{(e)} \sinh(\alpha_n^{(2)}y) + C_n^{(e)} \cosh(\alpha_n^{(2)}y)\} \cdot \sin(a_n x) \tag{2b}$$

Manuscript received August 18, 1975; revised October 27, 1975.
The authors are with the Department of Applied Electronics, University of Electro-Communications, Tokyo, Japan.

$$\psi_3^{(e)} = \sum_{n=1}^{\infty} D_n^{(e)} \sinh\{\alpha_n^{(3)}(b-y)\} \sin(a_n x) \quad (2c)$$

$$\psi_1^{(h)} = \sum_{n=0}^{\infty} A_n^{(h)} \cosh(\alpha_n^{(1)} y) \cos(a_n x) \quad (2d)$$

$$\psi_2^{(h)} = \sum_{n=0}^{\infty} \{B_n^{(h)} \cosh(\alpha_n^{(2)} y) + C_n^{(h)} \sinh(\alpha_n^{(2)} y)\} \cdot \cos(a_n x) \quad (2e)$$

$$\psi_3^{(h)} = \sum_{n=0}^{\infty} D_n^{(h)} \cosh\{\alpha_n^{(3)}(b-y)\} \cos(a_n x) \quad (2f)$$

where

$$a_n = \frac{n\pi}{a}$$

$$\alpha_n^{(i)} = \sqrt{a_n^2 + \beta^2 - k_i^2}, \qquad i = 1,2,3$$

and $A_n^{(e)}$, $B_n^{(e)}$, $C_n^{(e)}$, $D_n^{(e)}$, $A_n^{(h)}$, $B_n^{(h)}$, $C_n^{(h)}$, and $D_n^{(h)}$ are constants to be determined.

The boundary conditions of EM fields to connect these potentials are expressed as follows:

1) $y = h_1$

$$E_{z1} = E_{z2}, \qquad (0 \le x \le a) \quad (3a)$$

$$H_{z1} = H_{z2}, \qquad (0 \le x \le a) \quad (3b)$$

$$E_{x1} = E_{x2}, \qquad (0 \le x \le a) \quad (3c)$$

$$H_{x1} = H_{x2}, \qquad (0 \le x \le a). \quad (3d)$$

2) $y = h_1 + h_2$

$$E_{z2} = E_{z3}, \qquad (0 \le x \le a) \quad (4a)$$

$$E_{x2} = E_{x3}, \qquad (0 \le x \le a) \quad (4b)$$

$$E_{x2} = \begin{cases} f(x)e^{-j\beta z}, & (a_i'' \le x \le a_{i+1}', \\ & i = 0,1,\cdots,N, \text{ namely, on dielectrics}) \\ 0, & (a_i' \le x \le a_i'', \\ & i = 1,2,\cdots,N, \text{ namely, on conductors}) \end{cases} \quad (4c)$$

$$H_{x2} - H_{x3} = \begin{cases} 0, & (a_i'' \le x \le a_{i+1}', \\ & i = 0,1,\cdots,N) \\ g(x)e^{-j\beta z}, & (a_i' \le x \le a_i'', \\ & i = 1,2,\cdots,N) \end{cases} \quad (4d)$$

$$H_{z2} = H_{z3}, \qquad (a_i'' \le x \le a_{i+1}', \quad i = 0,1,\cdots,N) \quad (4e)$$

$$E_{z2} = 0, \qquad (a_i' \le x \le a_i'', \quad i = 1,2,\cdots,N). \quad (4f)$$

First, the EM fields in (1) are substituted for the boundary conditions in (3a)–(4d). By using the orthogonality of sinusoidal functions, the constants, $A_n^{(e)}$, $B_n^{(e)}$, $C_n^{(e)}$, $D_n^{(e)}$, $A_n^{(h)}$, $B_n^{(h)}$, $C_n^{(h)}$, $D_n^{(h)}$, can be derived as coefficients of the Fourier series expansion where, for simplicity, the following notations are defined:

$$F_n[f(\xi)] = \sum_{i=0}^{N} \int_{a_i''}^{a_{i+1}'} f(\xi) \cos(a_n \xi)\, d\xi \quad (5a)$$

$$G_n[g(\xi)] = \sum_{i=1}^{N} \int_{a_i'}^{a_i''} g(\xi) \sin(a_n \xi)\, d\xi. \quad (5b)$$

The rest of the conditions, (4e) and (4f), result in a set of homogeneous integral equations on the unknown functions, $f(\xi)$ $(a_i'' \le \xi \le a_{i+1}', i = 0,1,\cdots,N)$ and $g(\xi)$ $(a_i' \le \xi \le a_i'', i = 1,2,\cdots,N)$. Physically, $g(\xi)$ is proportional to the z directed electric currents on the boundary surface.

$$\sum_{n=0}^{\infty} \{P_n(\beta)F_n[f(\xi)] + R_n(\beta)G_n[g(\xi)]\} \cos(a_n x) = 0, \qquad (a_i'' \le x \le a_{i+1}', i = 0,1,\cdots,N) \quad (6a)$$

$$\sum_{n=0}^{\infty} \{R_n(\beta)F_n[f(\xi)] + Q_n(\beta)G_n[g(\xi)]\} \sin(a_n x) = 0, \qquad (a_i' \le x \le a_i'', i = 1,2,\cdots,N) \quad (6b)$$

where $P_n(\beta)$, $Q_n(\beta)$, and $R_n(\beta)$ are given in the Appendix.

III. Numerical Solutions by Nonuniform Discretization

The preceding simultaneous homogeneous integral equations (6) are numerically solved by the discretization of the integral regions, $\{0 \le \xi \le a_1', a_1' \le \xi \le a_1'', \cdots, a_N' \le \xi \le a_N'', a_N'' \le \xi \le a\}$, where the number of subregions are $\{M_0, M_1, \cdots, M_{2N}\}$, respectively, and the total number of subregions is M. When the functions to be solved, $f(\xi)$ and $g(\xi)$, are assumed to be constant in each subregion, the simultaneous integral equations (6) are rewritten as a set of simultaneous homogeneous linear equations with M variables. The determinant of these linear equations should vanish in order to have nontrivial solutions. The phase constant β can be calculated by solving this determinant equation.

The computation accuracy depends on the way of the discretization when the total number of subregions is fixed. We apply the nonuniform discretization method, which was developed in the TEM analysis of microstrip line [19], to the present case. There is a fact in the EM theory that fields vary very rapidly near strip-conductor edges. Therefore, our principle of the discretization is that the integral regions should be discretized more precisely when the considering point is closer to the edge. Fig. 2 shows an illustration of the uniform and nonuniform discretization methods. Fig. 3 shows the computation accuracy of the two discretization methods in the case of a shielded microstrip line. When the total number of subregions M is increased, the nonuniform discretization is seen to result in much faster convergence than the uniform discretization. The nonuniform discretization is employed throughout our work.

The numerical data obtained based on this method are compared with published data by other methods [8]–[11], in Fig. 4, and with those by empirical formulas [12]–[14], in Fig. 5. These curves indicate that our results are very close to those of Kowalski and Pregla (the mode-matching method) [11] in a wide range of frequencies. This agreement verifies the accuracy of the two methods. The empirical formulas in Fig. 5 seem to lose the accuracy at high frequencies.

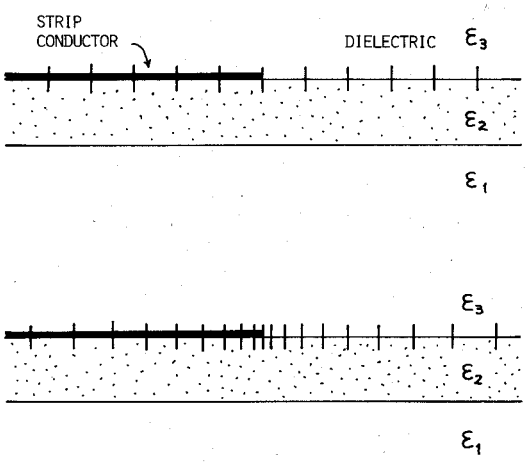

Fig. 2. Illustration of two discretization methods.

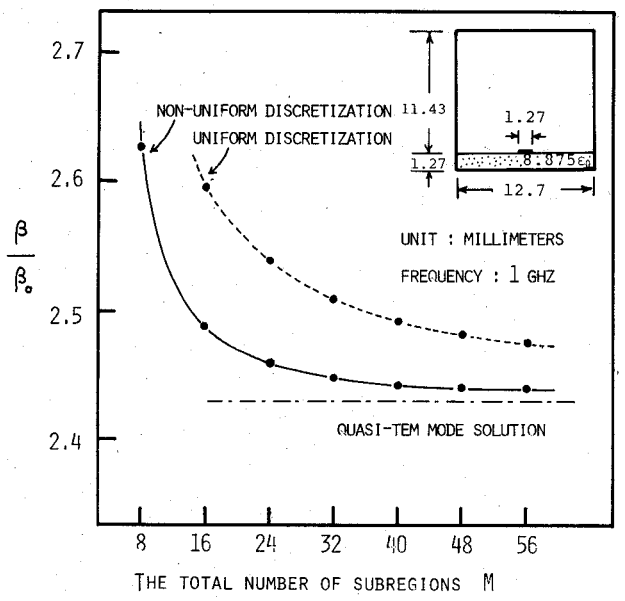

Fig. 3. The dependence of convergence on the way of the discretization.

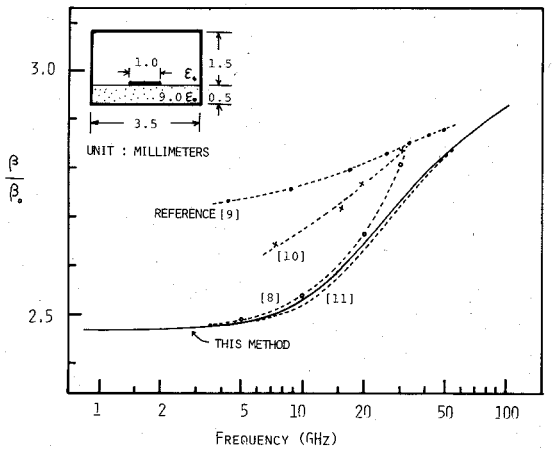

Fig. 4. The comparison of this method with other methods.

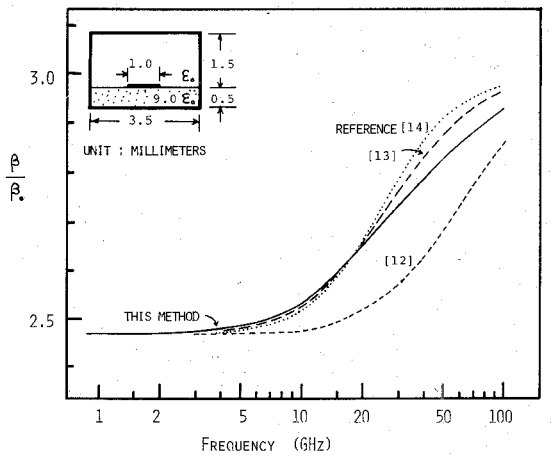

Fig. 5. The comparison of this method with empirical formulas.

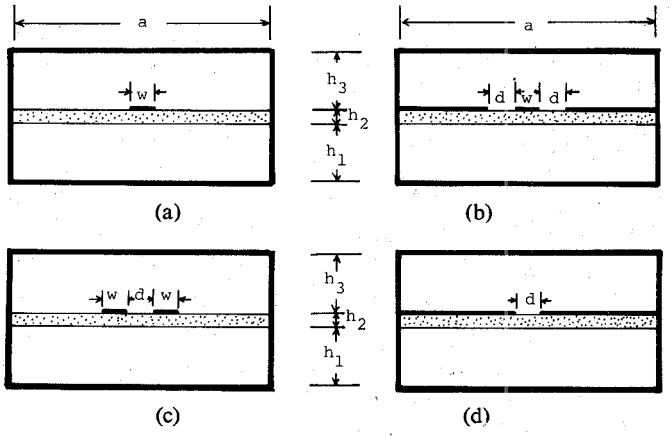

Fig. 6. Various shielded striplines with similar boundary conditions.

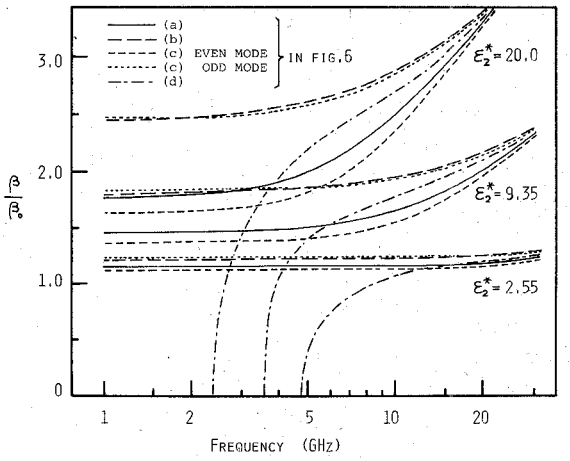

Fig. 7. The f–β characteristics of the structures in Fig. 6. a = 20 mm, $h_1 = h_3$ = 4.5 mm, h_2 = 1.0 mm, $w = d$ = 2.0 mm, $\varepsilon_1^* = \varepsilon_2^*$ = 1.0.

IV. Various Shielded Structures

The dispersion characteristics of the dominant mode of various shielded planar structures were investigated by the preceding method in a similar fashion. Fig. 6 shows the cross-sectional view of shielded transmission lines. Fig. 7 shows their characteristics for the cases, $\varepsilon_2^* = 2.55$,

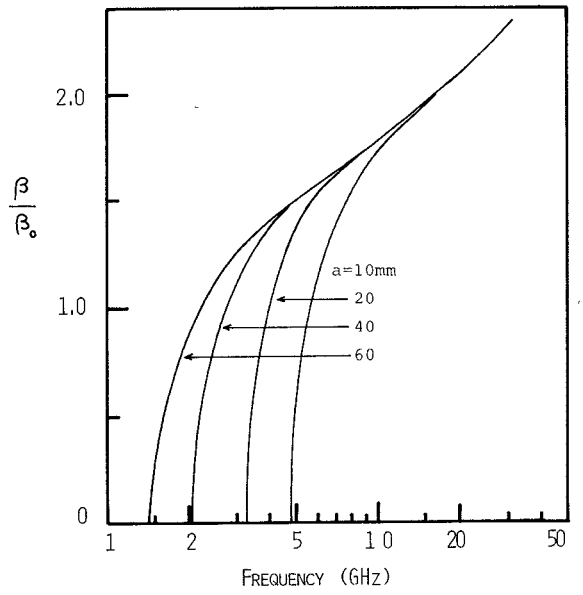

Fig. 8. The f–β characteristics of the shielded slot lines in Fig. 6(d). $h_1 = h_3 = 4.5$ mm, $h_2 = 1.0$ mm, $d = 2.0$ mm, $\varepsilon_1^* = \varepsilon_3^* = 1.0$, $\varepsilon_2^* = 9.35$.

$\varepsilon_2^* = 9.35$, and $\varepsilon_2^* = 20.0$. It is noted that the characteristics of the coplanar structure have a similarity to those of the odd-mode coupled microstrip line, and the slot line has a quite different nature from microstrip lines, though both are of the planar structure. Fig. 8 shows the dependence of the phase constant of the shielded slot lines in Fig. 6(d) on the frequency and the width of the shield conductor. It is seen that the phase constant is not much affected by the width in the high-frequency region since the EM field energy is concentrated around the slot at high frequencies.

V. Higher Order Modes of Shielded Microstrip Lines

This method was applied to the analysis of higher order modes of various structures. The cases of the shielded microstrip line, for example, are shown in Figs. 9–12. The longitudinal-section electric (LSE) and linear synchronous motor (LSM) modes of the two-medium waveguide in Fig. 9 are seen to be gradually changed to stripline modes when the center strip conductor appears and the strip width is increased.

By comparing Figs. 9 and 10, the following are observed.

1) The dominant mode close to the TEM solution appears in Fig. 10 because of the existence of the center conductor.

2) The degeneracies existing between even modes (solid lines) and between odd modes (dotted lines) in Fig. 9 have been resolved in Fig. 10. However, the degeneracies between even and odd modes in Fig. 9 have not been resolved in Fig. 10 because of the structural symmetry.

3) While the odd-mode characteristics in Fig. 9 are not much changed in Fig. 10, the even-mode characteristics are quite changed there.

When the characteristics of the lines with various strip widths are compared in Figs. 10–12, the following are observed with the increase of the width.

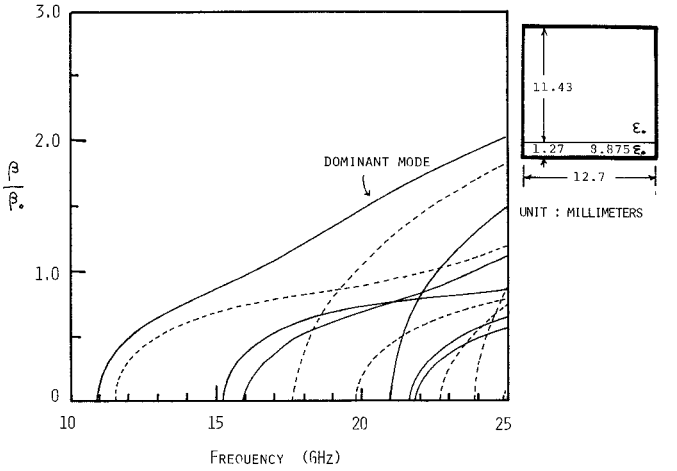

Fig. 9. The f–β characteristics of the LSE and LSM modes in a two-medium waveguide.

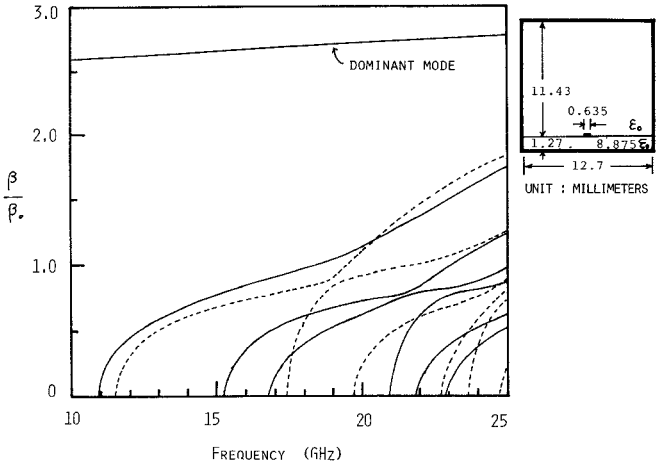

Fig. 10. The f–β characteristics of the shielded microstrip line with the strip width of 0.635 mm.

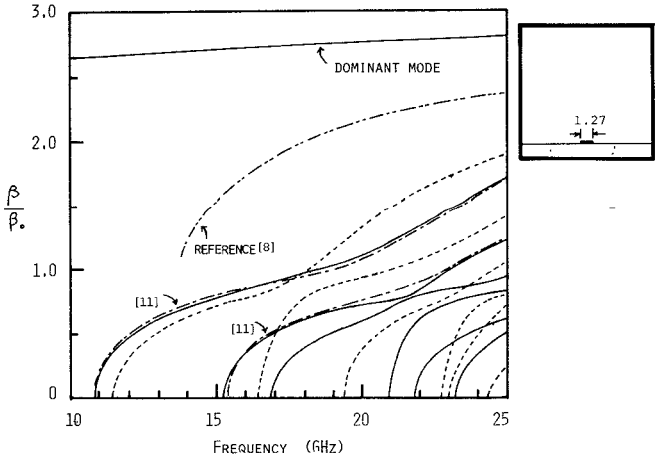

Fig. 11. The f–β characteristics of the shielded microstrip line with the strip width of 1.27 mm, compared with other available data.

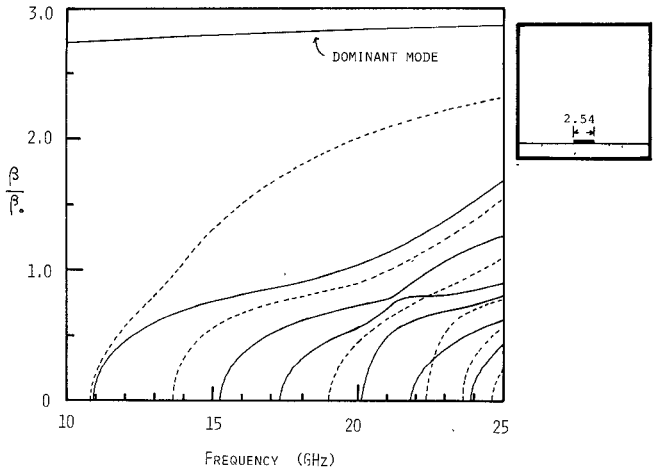

Fig. 12. The f–β characteristics of the shielded microstrip line with the strip width of 2.54 mm.

1) The phase constant of the dominant mode is gradually changed.

2) While the even-mode characteristics are not much changed, the odd-mode characteristics are changed rapidly.

3) The cutoff frequencies of the first- and the third-order mode of the shielded microstrip line are almost equal to the cutoff frequencies of the LSE and LSM modes of the corresponding two-medium waveguide.

4) The first higher order mode of the shielded microstrip line is the even mode when the strip is narrow, and the odd mode when the strip is wide.

Some of these numerical data are compared with other available data [8], [11] in Fig. 11. Again, our results are in good agreement with those of Kowalski and Pregla [11]. A small dip is noticed on the curve of the third higher order mode (solid line) at about 22 GHz in Fig. 11. The complexity of the phase constant curves for higher order modes such as this dip can be understood only by considering the resolution of waveguide-mode degeneracies as pointed out in the preceding.

VI. Conclusions

This paper described a method to analyze the microstrip-like transmission lines. The nonuniform discretization approach was found to be numerically effective in finding solutions of integral equations for the microstrip-like transmission lines. The results of computations in the case of the shielded microstrip line were very close to one of published data in a wide range of frequencies. The limitations of published empirical formulas at high frequencies were also recognized. Various planar transmission lines were compared to each other from the viewpoint of the f–β characteristics.

The higher order modes of the shielded microstrip lines were compared with those of the LSE and LSM modes. The observation on the similarity of cutoff frequencies between these modes may be useful to estimate the frequency range of the dominant mode of the microstrip line in a simple way. It was also found to be important to investigate the resolution process of waveguide-mode degeneracies due to the existence of a center strip conductor in order to explain the complex shape of the phase constant curves for higher order modes of microstrip lines.

Appendix

$P_n(\beta), R_n(\beta), Q_n(\beta)$ in (6) are given by

$$P_n(\beta) = \frac{\omega\mu_0}{\Delta_n}\left[\alpha_n^{(1)}\alpha_n^{(2)}\left\{\tanh^2(\alpha_n^{(1)}h_1) + \frac{\varepsilon_1}{\varepsilon_2}\tanh^2(\alpha_n^{(2)}h_2)\right\} + \left(\alpha_n^{(1)2} + \frac{\varepsilon_1}{\varepsilon_2}\alpha_n^{(2)2}\right)\tanh(\alpha_n^{(1)}h_1)\tanh(\alpha_n^{(2)}h_2)\right] \cdot \alpha_n^{(3)}\tanh(\alpha_n^{(3)}h_3)$$

$$R_n(\beta) = \frac{\beta a_n}{\Delta_n}\left[\left\{\alpha_n^{(2)}\tanh(\alpha_n^{(1)}h_1) + \frac{\varepsilon_1}{\varepsilon_2}\alpha_n^{(1)}\tanh(\alpha_n^{(2)}h_2) + \alpha_n^{(1)}\tanh^2(\alpha_n^{(1)}h_1)\tanh(\alpha_n^{(2)}h_2) + \alpha_n^{(2)} \cdot \left(\frac{\varepsilon_1}{\varepsilon_2} + \frac{k_2^2 - k_1^2}{\alpha_n^{(2)2}}\right)\tanh(\alpha_n^{(1)}h_1)\tanh^2(\alpha_n^{(2)}h_2)\right\} \cdot \alpha_n^{(3)}\tanh(\alpha_n^{(3)}h_3) + \alpha_n^{(1)}\alpha_n^{(2)} \cdot \left\{\tanh^2(\alpha_n^{(1)}h_1) + \frac{\varepsilon_1}{\varepsilon_2}\tanh^2(\alpha_n^{(2)}h_2)\right\} + \left(\alpha_n^{(1)2} + \frac{\varepsilon_1}{\varepsilon_2}\alpha_n^{(2)2}\right)\tanh(\alpha_n^{(1)}h_1)\tanh(\alpha_n^{(2)}h_2)\right]$$

$$Q_n(\beta) = \frac{1}{\Delta_n}\frac{k_2^2}{\omega\mu_0}\left[\left\{\frac{\varepsilon_1}{\varepsilon_2}\alpha_n^{(1)}\alpha_n^{(2)} + \left(\alpha_n^{(1)2} + \frac{\varepsilon_1}{\varepsilon_2}\alpha_n^{(2)2}\right) \cdot \tanh(\alpha_n^{(1)}h_1)\tanh(\alpha_n^{(2)}h_2) + \alpha_n^{(1)}\alpha_n^{(2)} \cdot \tanh^2(\alpha_n^{(1)}h_1)\tanh^2(\alpha_n^{(2)}h_2)\right\} \cdot \alpha_n^{(3)}\tanh(\alpha_n^{(3)}h_3) + \frac{\varepsilon_1}{\varepsilon_2}\alpha_n^{(1)}\left(\alpha_n^{(3)2} + \frac{\varepsilon_3}{\varepsilon_2}\alpha_n^{(2)2}\right)\tanh(\alpha_n^{(2)}h_2) + \alpha_n^{(2)}\left(\frac{\varepsilon_1}{\varepsilon_2}\alpha_n^{(3)2} + \frac{\varepsilon_3}{\varepsilon_2}\alpha_n^{(1)2}\right)\tanh(\alpha_n^{(1)}h_1) + \alpha_n^{(2)}\left(\frac{\alpha_n^{(1)2}}{\alpha_n^{(2)2}}\alpha_n^{(3)2} + \frac{\varepsilon_1\varepsilon_3}{\varepsilon_2^2}\alpha_n^{(2)2}\right) \cdot \tanh(\alpha_n^{(1)}h_1)\tanh^2(\alpha_n^{(2)}h_2) + \left(\alpha_n^{(3)2} + \frac{\varepsilon_3}{\varepsilon_2}\alpha_n^{(2)2}\right)\alpha_n^{(1)}\tanh^2(\alpha_n^{(1)}h_1) \cdot \tanh(\alpha_n^{(2)}h_2) + \frac{\varepsilon_3}{\varepsilon_2}\left\{\alpha_n^{(1)}\alpha_n^{(2)}\tanh^2(\alpha_n^{(1)}h_1) + \frac{\varepsilon_1}{\varepsilon_2}\alpha_n^{(1)}\alpha_n^{(2)}\tanh^2(\alpha_n^{(2)}h_2) + \left(\alpha_n^{(1)2} + \frac{\varepsilon_1}{\varepsilon_2}\alpha_n^{(2)2}\right)\tanh(\alpha_n^{(1)}h_1) \cdot \tanh(\alpha_n^{(2)}h_2)\right\}\alpha_n^{(3)}\coth(\alpha_n^{(3)}h_3)\right]$$

$$\Delta_n = \Bigg[\alpha_n^{(2)}(k_1^2 - a_n^2)\tanh(\alpha_n^{(1)}h_1) + \frac{\varepsilon_1}{\varepsilon_2}\alpha_n^{(1)} \cdot (k_2^2 - a_n^2)\tanh(\alpha_n^{(2)}h_2) + \alpha_n^{(1)}(k_2^2 - a_n^2)\tanh^2(\alpha_n^{(1)}h_1)\tanh(\alpha_n^{(2)}h_2) + \alpha_n^{(2)}\left\{\frac{\varepsilon_1}{\varepsilon_2}(k_2^2 - a_n^2) + \frac{\beta^2}{\alpha_n^{(2)2}}(k_2^2 - k_1^2)\right\} \cdot \tanh(\alpha_n^{(1)}h_1)\tanh^2(\alpha_n^{(2)}h_2)\Bigg]\alpha_n^{(3)}\tanh(\alpha_n^{(3)}h_3) + (k_3^2 - a_n^2)\Bigg[\alpha_n^{(1)}\alpha_n^{(2)}\left\{\tanh^2(\alpha_n^{(1)}h_1) + \frac{\varepsilon_1}{\varepsilon_2}\tanh^2(\alpha_n^{(2)}h_2)\right\} + \left(\alpha_n^{(1)2} + \frac{\varepsilon_1}{\varepsilon_2}\alpha_n^{(2)2}\right) \cdot \tanh(\alpha_n^{(1)}h_1)\tanh(\alpha_n^{(2)}h_2)\Bigg].$$

ACKNOWLEDGMENT

The authors wish to thank Professor T. Okabe for his helpful advice.

REFERENCES

[1] H. A. Wheeler, "Transmission-line properties of parallel strips separated by a dielectric sheet," *IEEE Trans. Microwave Theory Tech.*, vol. MTT-13, pp. 172–185, Mar. 1965.
[2] H. E. Green, "The numerical solution of some important transmission-line problems," *IEEE Trans. Microwave Theory Tech. (Special Issue on Microwave Filters)*, vol. MTT-13, pp. 676–692, Sept. 1965.
[3] E. Yamashita and R. Mittra, "Variational method for the analysis of microstrip lines," *IEEE Trans. Microwave Theory Tech.*, vol. MTT-16, pp. 251–256, Apr. 1968.
[4] P. Silvester, "TEM wave properties of microstrip transmission lines," *Proc. Inst. Elec. Eng.*, vol. 115, pp. 43–48, Jan. 1968.
[5] P. Daly, "Hybrid-mode analysis of microstrip by finite-element methods," *IEEE Trans. Microwave Theory Tech.*, vol. MTT-19, pp. 19–25, Jan. 1971.
[6] E. J. Denlinger, "A frequency dependent solution for microstrip transmission lines," *IEEE Trans. Microwave Theory Tech.*, vol. MTT-19, pp. 30–39, Jan. 1971.
[7] G. I. Zysman and D. Varon, "Wave propagation in microstrip transmission lines," in *1969 Int. Microwave Symp. Dig.* (Dallas, TX), pp. 3–9.
[8] R. Mittra and T. Itoh, "A new technique for the analysis of the dispersion characteristics of microstrip lines," *IEEE Trans. Microwave Theory Tech.*, vol. MTT-19, pp. 47–56, Jan. 1971.
[9] J. S. Hornsby and A. Gopinath, "Fourier analysis of a dielectric loaded waveguide with a microstrip line," *Electron. Lett.*, vol. 5, pp. 265–267, June 1969.
[10] ——, "Numerical analysis of a dielectric-loaded waveguide with a microstrip line—Finite-difference method," *IEEE Trans. Microwave Theory Tech.*, vol. MTT-17, pp. 684–690, Sept. 1969.
[11] G. Kowalski and R. Pregla, "Dispersion characteristics of shielded microstrips with finite thickness," *Arch. Elek. Ubertragung*, vol. 107, pp. 163–170, Apr. 1971.
[12] M. V. Schneider, "Microstrip dispersion," *Proc. IEEE*, vol. 60, pp. 144–146, Jan. 1972.
[13] W. J. Getsinger, "Microstrip dispersion model," *IEEE Trans. Microwave Theory Tech.*, vol. MTT-21, pp. 34–39, Jan. 1973.
[14] H. J, Carlin, "A simplified circuit model for microstrip," *IEEE Trans. Microwave Theory Tech.*, vol. MTT-21, pp. 589–591, Sept. 1973.
[15] C. P. Wen, "Coplanar waveguide: A surface strip transmission line suitable for non-reciprocal gyromagnetic device applications," *IEEE Trans. Microwave Theory Tech. (1969 International Microwave Symp.)*, vol. MTT-17, pp. 1087–1090, Dec. 1969.
[16] A. Torisawa, "The analysis and experiment on parallel triple strip line," B.S. thesis, Univ. Electro-Communications, Tokyo, Japan, Mar. 1969.
[17] S. B. Cohn, "Slot line on a dielectric substrate," *IEEE Trans. Microwave Theory Tech.*, vol. MTT-17, pp. 768–778, Oct. 1969.
[18] R. F. Harrington, *Time-Harmonic Electromagnetic Fields*. New York: McGraw-Hill, 1961.
[19] K. Atsuki and E. Yamashita, "Analytical method for transmission lines with thick-strip conductor, multi-dielectric layers and shielding conductor," *J. Inst. Electron. Commun. Eng. Jap.*, vol. 53-B, pp. 322–328, June 1970.
[20] E. Yamashita, "Variational method for the analysis of microstrip-like transmission lines," *IEEE Trans. Microwave Theory Tech.*, vol. MTT-16, pp. 529–535, Aug. 1968.
[21] K. Atsuki and E. Yamashita, "Higher order modes of microstrip lines" (in Japanese), presented at the Inst. Electron. Commun. Eng. Jap. Technical Group Meeting on Microwaves, Feb. 1974, Paper MW73-116.
[22] ——, "Dispersion characteristics of strip lines" (in Japanese), presented at the Inst. Electron. Commun. Eng. Jap. Technical Group Meeting on Microwaves, June 1974, Paper MW74-18.
[23] D. G. Corr and J. B. Davies, "Computer analysis of the fundamental and higher order modes in single and coupled microstrip," *IEEE Trans. Microwave Theory Tech.*, vol. MTT-20, pp. 669–678, Oct. 1972.